Research Article

Miao Yang, Xiaobo Liu*, Zhiyi Zhang, Yulai Song, and Lei Bai

Effect of Adding Rare Earth Elements Er and Gd on the Corrosion Residual Strength of Magnesium Alloy

https://doi.org/10.1515/phys-2019-0042
Received Apr 01, 2019; accepted Jun 04, 2019

Abstract: The effects of the single and compound addition of rare earth Gd and Er on corrosion resistance and residual strength of as-cast AM50 magnesium alloy were studied using XRD, SEM, EDS, the weightlessness test, electrochemistry method, and tensile test. The results of XRD and SEM showed that Al_3Er, Al_2Gd_3, and Al–Mn–Gd(Er) phases appeared in the alloy structure after the addition of rare earth Er and Gd. The results from the weightlessness test and Tafel curves show that the corrosion resistance of the modified composite rare earth was improved. Stress concentration caused by a corrosion pit is the direct cause of the tensile samples after corrosion. The corrosion residual strength of modified composite rare earth specimens is better than that of modified single rare earth samples. Fracture analysis indicates that the addition of rare earth elements did not change the fracture mechanism of the alloy, and the fracture was still the cleavage fracture.

Keywords: magnesium alloy; rare earth element Er; rare earth element Gd; corrosion residual strength

PACS: 81.70-q, 81.40 Np

1 Introduction

Mg alloys, as the lightest metal structures, are widely applied in the automotive and aerospace industries owing to their ultra-high specific strength and specific stiffness, excellent damping noise reduction, and liquid forming ability [1–3]. Mg alloys are also energy-saving, recyclable, and pollution-free, which attracts wide-spread global attention [4]. However, the application of Mg alloys is limited by their low corrosion resistance. Corrosion will gradually weaken the mechanical properties of Mg alloys, leading to sudden fracture and interfering with service life prediction. Thus, research on the rules of corrosion residual strength are particularly important and must be taken seriously.

Among different material performance improvement methods, alloying is frequently used, particularly alloying with rare earth elements (REEs) [5]. REEs belong to the IIIB family on the periodic table, and their outermost layers have the same electron structures containing two electrons, while the second outermost layers also have similar electron structures. However, the electron numbers on the 4f orbit of the third outermost layers vary from 0 to 14. REEs have similar and active chemical properties. Mg and REEs are both tightly arranged hexagonal structures, and the differences in atomic radius between them are within ±15%. Moreover, because of their similar electronegativity, REEs are all highly solid-soluble in Mg alloys. The addition of REEs, which possess very special physiochemical properties, refines the crystal grains and improves the structures, high-temperature mechanical properties, and corrosion resistance of Mg and its alloys [6–8]. In particular, REE Gd has an electron arrangement of $4f^7 5d^1 6s^2$, and a semi-full 4f electron orbit, forming a stable electron structure [9]. Because of the very large atomic radius and since the outermost-layer s electron and the single-layer 5d electron are prone to loss, Gd can become Gd^{3+} with high chemical activity. The Er atom has an outermost valence electron status of $4f^{12} 5d^1 6s^2$ and also belongs to trivalent REEs [11].

Thus far, Er or Gd have been used to modify Mg alloys [10–13]. For instance, the addition of 0.98–1.92% Er into AZ91 Mg alloys efficiently refined the crystal grains of as-cast alloys and improved the room-temperature tensile strength from 162 to 211 MPa [14]. The addition of 1% Gd significantly enhanced the corrosion resistance and

***Corresponding Author: Xiaobo Liu:** College of Mechanical Engineering, Beihua University, Jilin,132021, China;
Email: stone-666@126.com
Miao Yang: Engineering Training Center, Beihua University, Jilin, 132021, China, Email: yangmiao1021@163.com
Zhiyi Zhang, Lei Bai: Engineering Training Center Beihua University, Jilin, 132021, China
Yulai Song: College of Material Science and Engineering, Jilin University, Changchun 130022,China

tensile property of AM50 Mg alloys [15, 19]. REE modification methods include single-REE and multi-REE methods. Though single-REE modification has been proven to improve the corrosion resistance and mechanical performance of Mg alloys, the action mechanisms of multi-REE modification are still unclear. Multiple REEs play different roles in improving material properties [16, 17]. Thus, in this study, the effects of single or joint addition of Er and Gd on the corrosion resistance, mechanical properties, and residual strength of Mg alloys were investigated.

2 Materials and methods

2.1 Materials preparation

The designed compositions and names of the new alloys are listed in Table 1. Commercial AM50 alloy, industrial pure Al, Mg–Gd (20% wt. Gd), and Mg–Er (20% wt. Er) intermediate alloys were selected for alloy smelting. In addition, a small amount of aluminum was added because the desired material is 1% Gd/Er/Er + Gd and 99% AM50 magnesium alloy. However, the addition of Gd/Er required an Mg–Gd/Er intermediate alloy, which added more Mg and changed the content of Al in the AM50 magnesium alloy. Therefore, a small amount of Al was added to adjust the composition through calculation.

At the casting-stage, AM50 alloys were put into a high resistance furnace using a graphite crucible and remelted. Then, after the temperature rose to 720°C, the Mg–Gd/Mg–Er intermediate alloy and the pure Al were added into the molten AM50 metal liquids. The liquid was stirred for 5 min and homogenized for 20 min. At 710°C, the metal liquids were poured into a steel mold, which was preheated to 200°C. The size of the molds was 12 × 120 × 200 mm. The smelting proceeded under the protection of high-purity argon gas. The size of tensile specimens is illustrated in Figure 1, with reference to ASTM B557. The actual element contents of the alloy were detected by inductively coupled plasma atomic emission spectrometry (ICP-AES) and are listed in Table 2.

Table 1: Design compositions and names of experimental alloy (wt%)

Name of sample alloy	Gd	Er	AM50
AM50Er	0	1	Bal.
AM50Gd	1	0	Bal.
AM50ErGd	1	1	Bal.

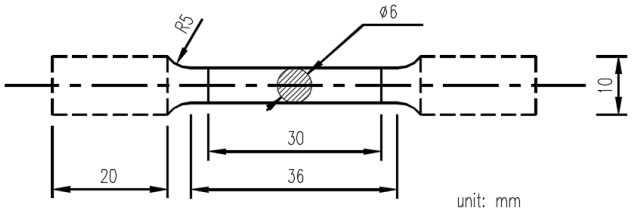

Figure 1: Schematic drawing of the tensile test sample

2.2 Corrosion tests

The immersed corrosion tests were performed in a 3.5% wt. NaCl saturated $Mg(OH)_2$ solution, which was prepared with analytically pure reagents and distilled water. In brief, a 3.5% NaCl solution was first prepared, then Mg $(OH)_2$ powder was added under continual stirring until powder precipitates appeared. The final solution was maintained at a pH of approximately 10.5, which ensured that the corrosion rate was unaffected by the pH of the corrosion solution. The solution corrosion tests were conducted in a constant-temperature incubator, which was maintained at 25°C. The specimens were first surface-polished with 1000 grit waterproof abrasive paper and then immersed into the corrosion solution. The corrosion time was set at 12, 24, 72, 168, 336, and 432 h. At each time point, three specimens were taken out and the surface corroded products were washed with a chromic silver nitrate solution (*i.e.*, 20 g of CrO_3 and 1 g of $AgNO_3$ dissolved in 100 ml of distilled water) and then washed under ultrasonic waves and with alcohols. After blow drying, the specimens were stored in bags.

The corrosion weight loss was measured using a 1/10000 electronic balance, and the corrosion rate was calculated as follows.

$$v_t = \frac{m_0 - m_t}{t \cdot S}(mg \cdot h^{-1} \cdot cm^{-2})$$

where m_0 and m_t were the specimen weights before and after erosion, respectively (mg); t was the erosion time in hours; and S (= 6.4 cm^3) was the specimen area.

Tafel curves were measured in 3.5% NaCl aqueous solution using electrochemical workstation LK98B II (Tianjin Lanlike Chemical Electronic High-Tech Co. LTD, Tianjin, China). The scan rate was 10 mV/s. The sample was used as the working electrode, the saturated calomel electrode used as the reference electrode, and platinum electrode used as the standard electrode.

Table 2: Actual element contents of alloys (wt%)

Name of sample alloy	Al	Gd	Er	Mn	Zn	Si	Cu	Ni	Mg
AM50Er	4.8961	0	0.9351	0.2849	0.1298	0.0136	0.0016	0.0010	Bal.
AM50Gd	4.8612	0.9172	0	0.2783	0.1234	0.0133	0.0013	0.0012	Bal.
AM50ErGd	4.8664	0.9097	0.9123	0.2818	0.1228	0.0133	0.0010	0.0010	Bal.

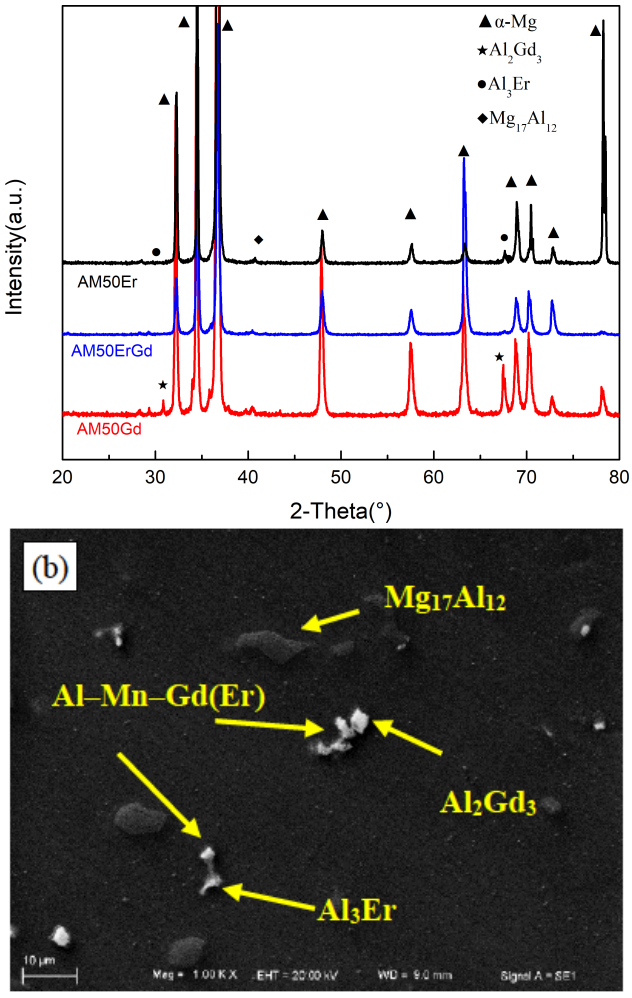

Figure 2: (a) XRD patterns from AM50Er, AM50ErGd, and (b) AM50Gd SEM micrographs of the microstructure of AM50ErGd magnesium alloys

2.3 Microstructure analysis

The specimens were characterized on a D/Max 2500 PC X-ray diffraction (XRD) machine using a Cu-Kα radiation target. The working voltage was 50 kV and the working current was 20 mA. The structures, elements, and fractures of the specimens were observed under a scanning electron microscope (SEM) (ZEISS EVO18, Germany) equipped with an energy dispersive spectrometer (EDS). The corroded macroscopic morphologies were photographed using a Canon camera.

2.4 Mechanical properties

Tensile strength was measured on an AG-10 universal tensile tester at a tensile rate of 1 mm/min. Residual strength was tested in triplicate and the minimum residual strength among the three specimens at the same corrosion time was selected.

3 Results and discussion

3.1 Structures

Figure 2a shows the XRD patterns of the alloys. Due to the low content of the major element Al (about 5%) in AM50 and only trace Er and Gd being added, the XRD patterns showed peaks of β-$Mg_{17}Al_{12}$, Al_2Gd_3, and Al_3Er in addition to α-Mg. After the joint addition of Er and Gd, all characteristic peaks appeared, but the peak of β-$Mg_{17}Al_{12}$ was weakened. This was mainly because the REEs robbed Al from β-$Mg_{17}Al_{12}$, leading to the reduced amount of β-$Mg_{17}Al_{12}$.

The microstructures of AM50ErGd clearly contained dark α-Mg; a bigger, greyish white island-like β-$Mg_{17}Al_{12}$; white, brighter, and smaller Al_2Gd_3, Al_3Er, and Al–Mn–Er(Gd); and other REE-enriched phases (Figure 2b). The EDS results of the phases are illustrated in Figure 3. According to previous research [6, 18], the addition of Gd into AM50 led to the formation of Al_2Gd_3 and Al–Mn–Gd, while the addition of Er resulted in the appearance of Al_3Er and Al–Mn–Er. The joint addition of Er and Gd did not induce any new phases, but only the REE-enriched phases appeared after the single addition of Er or Gd. Moreover, the REE-enriched phases were small-volumed and mutually accompanying. This was because of the thermodynamic conditions during the solidification of AM50 added with trace REEs, as the enrichment of the solute element led to the accompaniment of Al_2Gd_3, Al_3Er, and Al–Mn–Er(Gd).

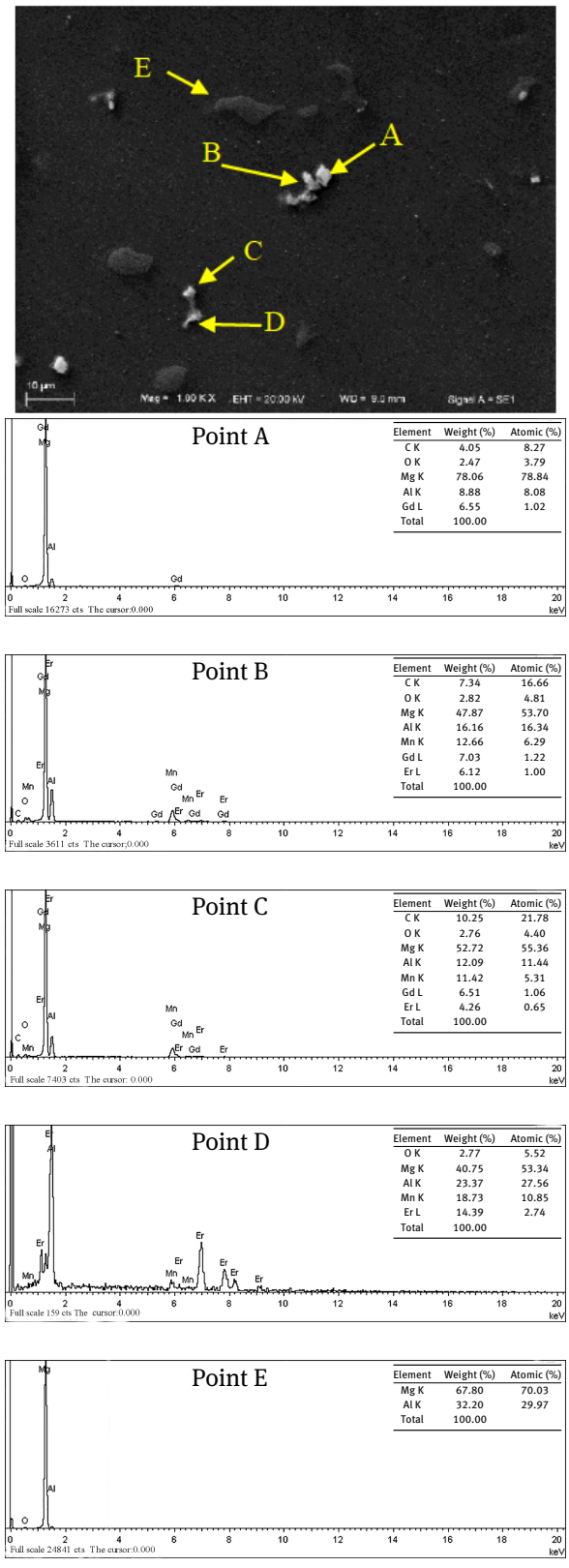

Figure 3: EDS results of Point A, B, C, D, and E

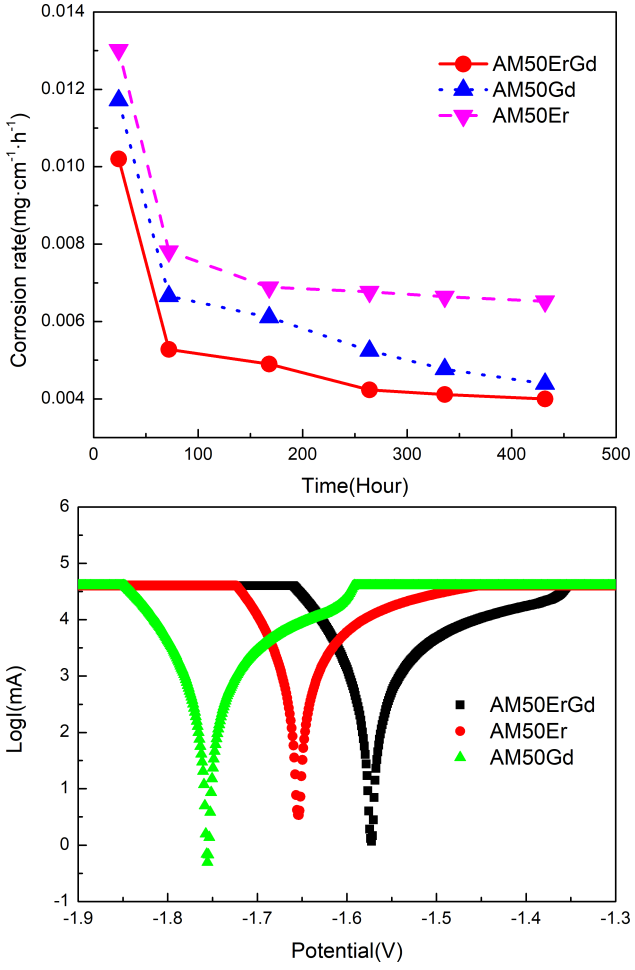

Figure 4: (a) Weight loss corrosion rate result and (B) Tafel curves of AM50Er, AM50Gd, and AM50ErGd magnesium alloy in 3.5% NaCl solution

3.2 Corrosion resistance

Figure 4a shows the weight loss corrosion rate curves of AM50Er, AM50ErGd, and AM50Gd in the 3.5% NaCl solution. According to the corrosion weight loss standard, the corrosion rates ranked as AM50Er > AM50Gd > AM50ErGd. The trends of the three curves were similar, as the corrosion rates all rapidly declined before 100 h but changed gradually after 100 h. After 100 h, the corrosion rate of AM50Er was approximately 0.007 $mg{\cdot}cm^{-1}{\cdot}h^{-1}$, that of AM50Gd declined from 0.0065 to 0.0042 $mg{\cdot}cm^{-1}{\cdot}h^{-1}$, and that of AM50ErGd decreased to 0.004 $mg{\cdot}cm^{-1}{\cdot}h^{-1}$. After the single addition of Gd, the corrosion rate declined relative to that after a single addition of Er. The corrosion rate after the joint addition of two elements was in between the two single-REE modified alloys, indicating that Gd improved the corrosion resistance of AM50 more than Er. This was mainly because Gd could purify the melts and

Table 3: The corrosion current density and corrosion potential of AM50Er, AM50Gd, and AM50ErGd magnesium alloy in 3.5% NaCl solution

Name of sample alloy	Corrosion Potential (V)	Corrosion Current density (mA)
AM50Er	−1.65	169.82
AM50Gd	−1.75	74.13
AM50ErGd	−1.57	50.11

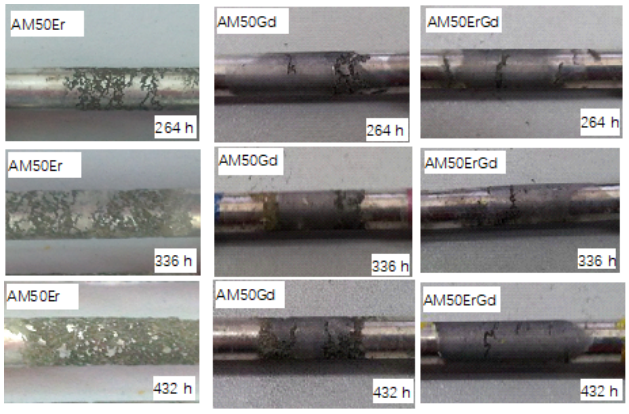

Figure 5: Microscope corrosion morphologies at 264, 336, and 432 h of AM50Er, AM50Gd, and AM50ErGd magnesium alloys

interact with Al to form Al_2Gd_3, which deprived Al from β-$Mg_{17}Al_{12}$and led to a reduction in the number of active micro-thermocouple pairs. Moreover, the resulting Al–Gd phase was an inert cathode that enhanced the corrosion resistance of the alloys.

Figure 4b displays the Tafel curves of AM50Er, AM50ErGd, and AM50Gd in 3.5% NaCl solution. Furthermore, the corrosion current density and corrosion potential according to the Tafel curves are illustrated in Table 3. The corrosion potential of AM50Er was −1.65V, and the corrosion current density was 169.82 mA. With Gd added of Gd, the corrosion potential increased to −1.57 V while the corrison current density decreased to 50.11 mA. Without Er, the corrosion potential of AM50Gd became negative (−1.75 V), and the corrosion current density increased to 169.82 mA. The results were also consistent with the weight loss results in Figure 4a.

Figure 5 shows the surface morphologies of AM50Er, AM50Gd, and AM50ErGd tensile rods after 264, 336, or 432 h of corrosion. Clearly, neither the single addition of Er/Gd nor the joint addition of Er and Gd prevented pit corrosion, which is the typical corrosion form of Mg alloys. With an increased immersion time, the corrosion in the two materials was intensified, the corroded areas were gradually enlarged, and the amount of eroded pits increased. However, at the same erosion time, the corrosion of the joint-modified Mg alloys was less severe than the single-REE modified Mg alloys, and the number of eroded pits decreased, indicating that the addition of Er and Gd also could enhance the corrosion resistance of the alloys. The corrosion rate of samples with Er alone was higher than that with Gd alone, which are consistent with Figure 4. Since Er is a surfactive element, its addition into alloys improved the quality and density of the corroded surface films and prevented Cl^- from destroying the films. However, compared to Gd, the Al–Er phase was more active than that of Al–Gd. This led to a slightly worse corrosion resistance of AM50Er compared to that of AM50Gd.

3.3 Mechanical properties

Figure 6 shows the engineering strain–stress curves and maximum tensile stress and elongation of AM50Gd, AM50Er, and AM50ErGd. Clearly, the tensile strengths of the AM50Gd, AM50Er, and AM50ErGd were 213, 216 and 218 MPa, respectively, not showing significant differences. Their elongation rates were 10.2%, 15.1%, and 13.7%, respectively, showing large differences. The elongation rate of the joint-modified alloy was in between the two single-REE-modified alloys. Comparison showed that Gd did not largely affect the elongation rates of the alloys but mainly enhanced the corrosion resistance, while Er mainly enhanced mechanical properties. Er could improve mechanical properties mainly because Er interacted with the Al in the alloys to form Al_3Er, which has a very strong Al–Er covalent bond that helped stabilize the crystal boundaries and maintain the high mechanical properties.

Figure 7 shows the fracture SEM images of the alloys. Clearly, Al–Er (Al–Mn–Er) particles were found in the dimples of AM50Er, and some even cracked (Figure 7a). Also, river-like patterns and torn edges were found, indicating they were intragranular fractures. The fracture image of AM50Gd (Figure 7b) was similar to that of AM50Er. However, the dimples were fewer, there were more cleavage steps, and they contained microcracks. The fracture image of AM50ErGd mainly showed torn edges and river-like patterns (Figure 7c), indicating they were intergranular fractures. The magnified image also showed cracks on the cleavage steps and the Al–Er(Gd) particles (Figure 7d).

The fracture morphology of the above three alloys was in accordance with the property data in Figure 6. The fracture mode was still quasi-cleavage fracture after the addition of Er and/or Gd into AM50. The only difference was that, after the single addition of Er, the number of dimples in the fractures increased and the alloys were tough-

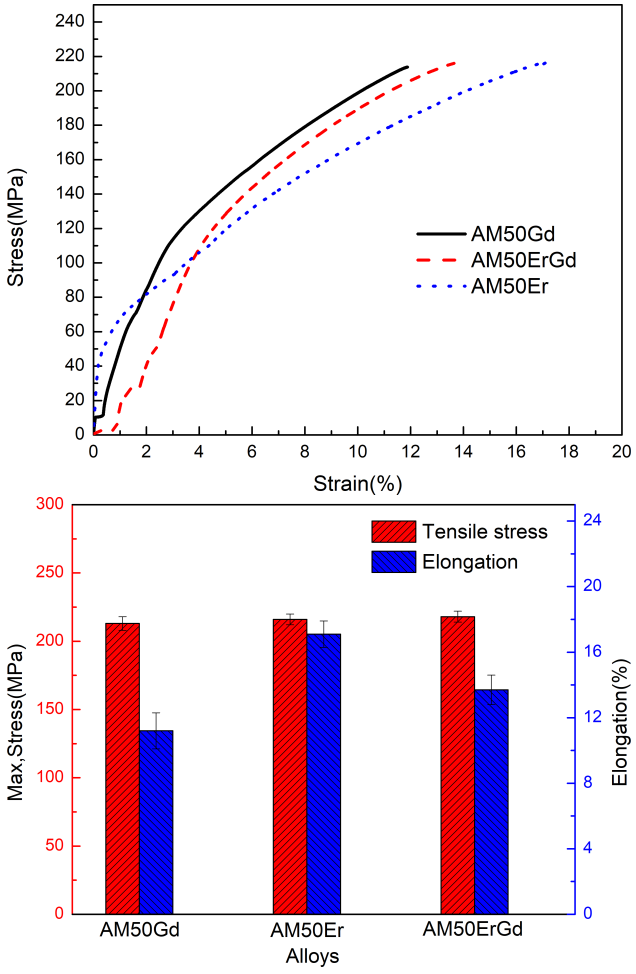

Figure 6: (a) The engineering strain-stress curves and (b) maximum tensile stress and elongation of AM50Gd, AM50Er, and AM50ErGd magnesium alloys

ened. After the single addition of Gd, the number of dimples decreased and the fractures mainly consisted of cleavage steps. After the joint addition of Er and Gd, the numbers of dimples and torn edges were both in between the two single-REE modified alloys.

3.4 Corrosion Residual strength (CRS)

As reported [19], the corroded strength was defined as the corrosion residual strength (CRS). Studying the rules of residual strength facilitates the prediction of service life and is thus very important.

Figure 8 shows the CRS curves of AM50Gd, AM50Er, and AM50ErGd. The residual strength ranks as AM50ErGd > AM50Gd > AM50Er, which is consistent with the corrosion resistance results.

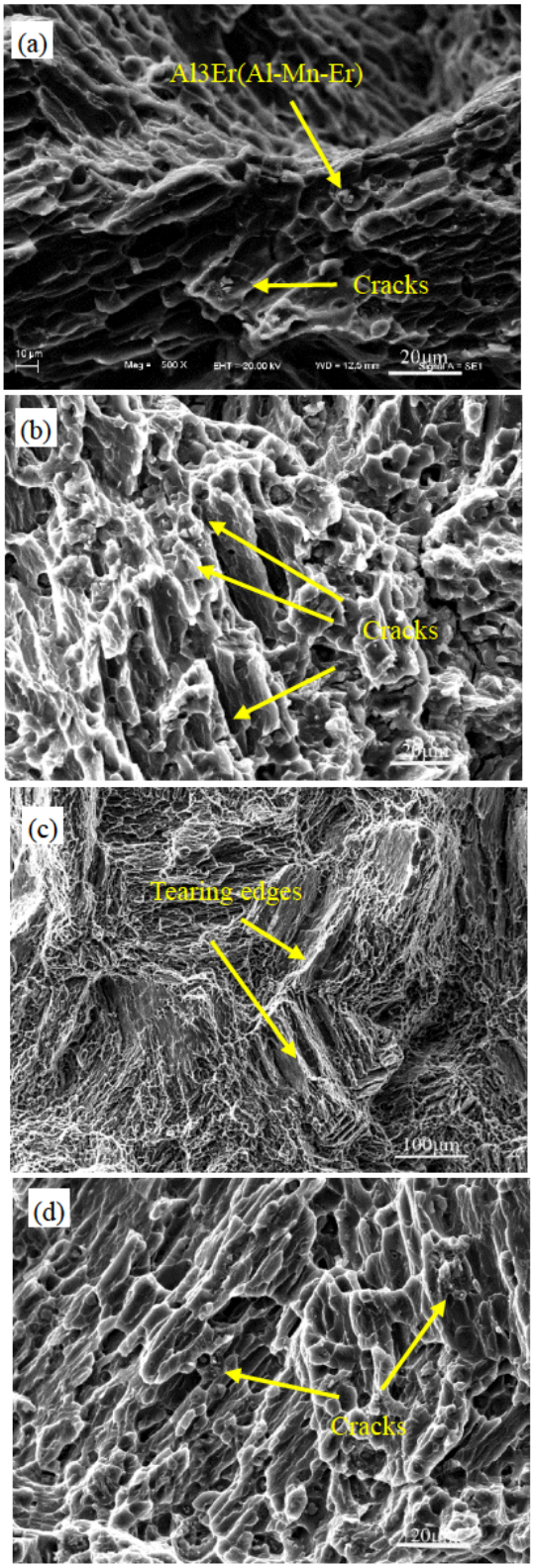

Figure 7: SEM images of tensile fracture morphology of (a) AM50Er, (b) AM50Gd, (c, d) AM50ErGd

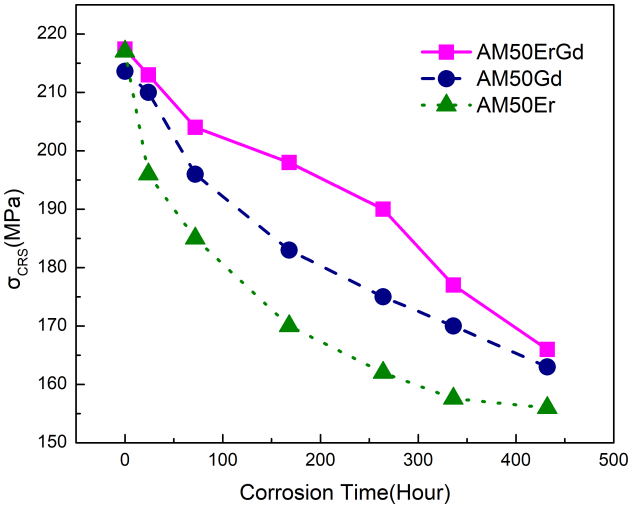

Figure 8: CRS curves of AM50Gd, AM50Er, and AM50ErGd magnesium alloys

The results of the original mechanical properties showed that the non-eroded strength did not differ largely among the three alloys, but the presence of Er and Gd improved the corrosion resistance and thereby increased the residual strength of AM50ErGd. Furthermore, the residual strength curve departed from the rules of negative exponential functions and were convexed forward. In comparison, the residual strength of the two single-REE-modified alloys still obeyed the rules of negative exponential functions. The joint modification of Er and Gd could better improve the corrosion resistance than the mechanical properties, which resulted from the joint action between Er and Gd.

During corrosion, the Mg alloys were affected by both internal factors (*e.g.*, alloy composition, structure) and external factors (*e.g.*, the erosion liquid). In this study, the internal influence factors were the phase composition and crystal grain size of alloys. After the addition of Er and/or Gd, new phases of Al–Er(Gd) and Al–Mn–Er(Gd) appeared. Since the second phase reinforcement improved the mechanical properties and new phases deprived Al from β-$Mg_{17}Al_{12}$, the amount of effective cathodal β-$Mg_{17}Al_{12}$ decreased and the erosion resistance was thereby enhanced. Since the alloys were eroded in Cl^--containing solutions due to the small radius of Cl^- and the loose surface structure of AM50 (*i.e.*, numerous hollows), the Cl^- could easily pass through the eroded films and approach the alloy surfaces, thereby severely eroding the Mg alloys. After the addition of Er and/or Gd, however, these REEs could enhance the quality of surface films in the AM50 alloys and relieve the impact of Cl^- onto the alloy surfaces.

Mg alloys are pit-eroded in Cl^--containing solutions, and pit erosion is the direct cause for the reduction of residual strength. For pit-eroded specimens during the tension process, the presence of eroded pits led to stress concentration, which resulted in rapid crack propagation and, finally, in fractures. Though the erosion reduced the effective diameter of the tensile specimens, it also decreased the residual strength, albeit not largely.

4 Conclusions

A comparative study of corrosion and mechanical properties by individual and compound additions of rare earth elements Er and Gd into AM50 was conducted. The main conclusions are as follows.

1) The joint addition of Er and Gd led to the formation of new Al_3Er, Al_2Gd_3, and Al–Mn–Gd(Er) phases in the alloys.
2) The corrosion weight loss results showed the corrosion rates ranked as AM50Er > AM50Gd > AM50ErGd.
3) Fracture analysis showed that the addition of REEs did not alter the fracturing mechanism, which was still quasi-cleavage fracturing.
4) The double-REE-modified alloys had higher residual strength than the single-REE modified alloys.
5) The stress concentration caused by eroded pits was the direct cause for the failure of residual strength alloys.

Acknowledgement: This study was supported by the National Natural Science Foundation of China (No. 51201068), Science and Technology Development Projects of Jilin Province (No. 201201032), National Natural Science Foundation Regional Science Foundation Project (No. 51564005), Jilin Science and Technology Innovation Development Plan Project (No. 201750247 and 201750225), and the Science and Technology Research Project of Education Department of Jilin Province (JJKH20180335KJ).

References

[1] Ding Y., Wen C., Hodgson P., Li Y., Effects of alloying elements on the corrosion behavior and biocompatibility of biodegradable magnesium alloys: a review, J Mater. Chem. B, 2014, 2,1912-1933.
[2] Liu W., Cao F., Zhong L., Zheng L., Jia B., Zhang Z., Zhang J., Influence of rare earth element Ce and La addition on corrosion behavior of AZ91 magnesium alloy, Mater. Corros., 2015, 60, 795-

803.
[3] Yang M., Liu X., Zhang Z., Song Y., Stress corrosion behavior of AM50Gd magnesium alloy in different environments, Metals, 2019, 9, 616-628.
[4] Song G., Bowles A.L., Stjohn D.H., Corrosion resistance of aged die cast magnesium alloy AZ91D, Mat. Sci. Eng. A, 2004, 366, 74-86.
[5] Liu W., Cao F., Chang L., Zhang Z., Zhang J., Effect of rare earth element Ce and La on corrosion behavior of AM60 magnesium alloy, Corros. Sci., 2009, 51, 1334-1343.
[6] Yang M., Zhang Z., Liu Y., Han X., Corrosion and mechanical properties of AM50 magnesium alloy after modified by different amounts of rare earth element Gadolinium, Open Phys., 2016, 14, 444-451.
[7] Yang M., Zhang Z., Han X., Liu Y., Corrosion mechanical properties of hot extrusion treated AM50GdX magnesium alloy, Chin. Rare Earth Soc., 2016, 34, 425-431.
[8] Zhang T., Li Y., 4 – Role of structure and rare earth (RE) elements on the corrosion of magnesium (Mg) alloys, Corros. Magnesium Alloys, 2011, 2011: 166-206.
[9] Wang W., Wu G., Wang Q, Huang Y., Ding W., Gd contents, mechanical and corrosion properties of Mg-10Gd-3Y-0.5Zr alloy purified by fluxes containing $GdCl_3$ additions, Mater. Sci. Eng. A 2009, 507, 207-214.
[10] Kruger J., Magnesium Alloys: Corrosion, Encyclopedia Mater. Sci. Technol., 2001, 4744-4745.
[11] Rosalbino F., Angelini E., De Negri S., Saccone A., Delfino S., Effect of erbium addition on the corrosion behaviour of Mg–Al alloys, Intermetallics, 2005, 13, 55-60.
[12] Rosalbino F., Angelini E., De Negri S., Saccone A., Delfino S., Influence of the rare earth content on the electrochemical behaviour of Al–Mg–Er alloys, Intermetallics, 2003, 11, 435-441.
[13] Wang Z., Jia W., Cui J., Study on the deformation behavior of Mg-3.6% Er magnesium alloy, J. Rare Earths, 2007, 25, 744-748.
[14] Xiao D.,Huang B., Effect of Erbium addition on microstructure and mechanical properties of as-cast AZ91 magnesium alloy, J. Chin Rare Earth Soc., 2008, 26,78-81.
[15] Yang M., Liu Y., Liu J., Song Y., Corrosion and mechanical properties of AM50 magnesium alloy after being modified by 1 wt.% rare earth element gadolinium, J. Rare Earth, 2014, 32, 558-563.
[16] Liu W., Cao F., Zhong L., Zheng .L, Jia B., Zhang Z., Zhang J., Influence of rare earth element Ce and La addition on corrosion behavior of AZ91 magnesium alloy, Corro. Sci., 2009, 60, 795-803
[17] Song Y., Wang Z., Liu Y., Yang M., Qu Q., Influence of Erbium, Cerium on the stress corrosion cracking behavior of AZ91 alloy in humid atmosphere, Adv. Eng. Mater., 2017, 19, 1700021.
[18] Yang M., Liu Y., Liu J., Zhang .Z, Jin C., Corrosion properties of AM50 magnesium alloy after 1% Er modified, Chin. Rare Earth., 2018, 39, 142-148.
[19] Li C., Liu Y., Wang Q., Zhang L., Zhang D., Study on the corrosion residual strength of the 1.0 wt.% Ce modified AZ91 magnesium alloy, Mater. Charact., 2010, 61, 123-127.